



**HAL**  
open science

## Transition from wave turbulence to dynamical crumpling in vibrated elastic plates

Benjamin Miquel, Alexandros Alexakis, Christophe Josserand, Nicolas Mordant

► **To cite this version:**

Benjamin Miquel, Alexandros Alexakis, Christophe Josserand, Nicolas Mordant. Transition from wave turbulence to dynamical crumpling in vibrated elastic plates. *Physical Review Letters*, 2013, pp.054302. 10.1103/PhysRevLett.111.054302. hal-01009494

**HAL Id: hal-01009494**

**<https://hal.science/hal-01009494v1>**

Submitted on 23 Nov 2023

**HAL** is a multi-disciplinary open access archive for the deposit and dissemination of scientific research documents, whether they are published or not. The documents may come from teaching and research institutions in France or abroad, or from public or private research centers.

L'archive ouverte pluridisciplinaire **HAL**, est destinée au dépôt et à la diffusion de documents scientifiques de niveau recherche, publiés ou non, émanant des établissements d'enseignement et de recherche français ou étrangers, des laboratoires publics ou privés.

## Transition from Wave Turbulence to Dynamical Crumpling in Vibrated Elastic Plates

Benjamin Miquel and Alexandros Alexakis

*Laboratoire de Physique Statistique, Ecole Normale Supérieure, Université Pierre et Marie Curie, CNRS, 24 rue Lhomond, 75005 Paris, France*

Christophe Josserand

*Institut d'Alembert, UMR 7190, CNRS and Université Pierre et Marie Curie, 4 Place Jussieu, 75005 Paris, France*

Nicolas Mordant\*

*Laboratoire des Écoulements Géophysiques et Industriels, Université Grenoble Alpes, Domaine Universitaire, BP53, 38041 Grenoble, France and Institut Universitaire de France, 103, Boulevard Saint-Michel, 75005 Paris, France*

(Received 2 April 2013; revised manuscript received 31 May 2013; published 2 August 2013)

We study the dynamical regime of wave turbulence of a vibrated thin elastic plate based on experimental and numerical observations. We focus our study on the strongly nonlinear regime described in a previous Letter by Yokoyama and Takaoka. At small forcing, a weakly nonlinear regime is compatible with the weak turbulence theory when the dissipation is localized at high wave number. When the forcing intensity is increased, a strongly nonlinear regime emerges: singular structures dominate the dynamics at large scales whereas at small scales the weak turbulence is still present. A turbulence of singular structures with folds and  $D$  cones develops that alters significantly the energy spectra and causes the emergence of intermittency.

DOI: [10.1103/PhysRevLett.111.054302](https://doi.org/10.1103/PhysRevLett.111.054302)

PACS numbers: 46.40.-f, 05.45.-a, 62.30.+d

A large ensemble of weakly nonlinear waves can develop a state of turbulence for which analytical derivations of the energy transfer can be performed: the weak (or wave) turbulence theory (WTT). Because of the hypothesis of weak nonlinearities, the statistics remain close to Gaussian and the WTT enables us to compute the so-called kinetic equation for the evolution of the spectral content of energy. The theory is appealing in the perspective of the theoretical study of turbulence in general because exact solutions of out-of-equilibrium dynamics can be derived analytically. These solutions show an energy flux between the large forcing scales and the small dissipation scales analogous to the Kolmogorov similarity solution for hydrodynamic turbulence [1–3].

Vibrating elastic plates are a fruitful models for wave turbulence study. WTT has been applied to this case in Ref. [4] and advanced measurements have been implemented that provided unprecedented results [5–10]. The normal deformation of thin elastic plates follows the Föppl-von Kármán equations [11,12]:

$$\rho \frac{\partial^2 \zeta}{\partial t^2} = - \frac{Eh^2}{12(1-\nu^2)} \Delta^2 \zeta + \mathcal{L}(\chi, \zeta), \quad (1)$$

$$\Delta^2 \chi = - \frac{E}{2} \mathcal{L}(\zeta, \zeta), \quad (2)$$

where  $\zeta$  is the transverse displacement,  $\chi$  the Airy stress function,  $h$  the thickness,  $\rho$  the density,  $E$  Young's modulus, and  $\nu$  the Poisson ratio. The operator  $\mathcal{L}$  is bilinear symmetric defined in Cartesian coordinates

by  $\mathcal{L}(f, g) = (\partial^2 f / \partial x^2)(\partial^2 g / \partial y^2) + (\partial^2 f / \partial y^2)(\partial^2 g / \partial x^2) - 2(\partial^2 f / \partial x \partial y)(\partial^2 g / \partial x \partial y)$ . The theory predicts an energy cascade from the forcing large scale to the small dissipative one, the so-called Kolmogorov-Zakharov (KZ) spectrum, following for the energy density

$$E_\zeta(k) = k \langle |\zeta_{\mathbf{k}}|^2 \rangle = C \frac{P^{1/3} \rho^{1/6}}{(12(1-\nu^2))^{1/6} E^{1/2}} \frac{\ln^{1/3}(k_*/k)}{k^3} \quad (3)$$

with  $\zeta_{\mathbf{k}}$  being the Fourier transform of the displacement,  $P$  the energy flux within the cascade, and  $k^*$  a cutoff scale related to the dissipation process [4].

While such scaling has been observed in numerical simulations where the dissipation is concentrated at small scales [4], experiments have shown a different behavior following approximately  $E_k \propto P^{0.6} k^{-3.5}$  [5,6]. Such discrepancy between the WTT and the experiments is mostly due to the real dissipation that is present at every scale so that no truly transparent window is present [13,14].

Recently, numerical studies have shown that a new strongly nonlinear regime emerges for intense forcing [15]. In fact, when the forcing increases, one expects that the assumption of weak nonlinearities fails, either at large or small scales, leading *a priori* to a new dynamics [16,17]. Such regime is hard to handle and no general theory exists yet. For instance, in systems allowing an inverse cascade, a condensate can develop that strongly alters the direct energy transfer [18]. For water waves, new regimes of turbulence have been identified for various forcing amplitudes [19]. Here we report experimental and numerical studies of this new regime. We show that intermittency appears at

strong forcing and that it can be attributed to the existence of singular structures in the wave field.

*Experiment.*—The experimental setup and the presented data set are the same as those of Ref. [10]. A stainless steel plate  $2 \times 1 \text{ m}^2$  and  $h = 0.4 \text{ mm}$  thick is held freely hanging from a beam. Vibrations are excited at 30 Hz by an electromagnetic shaker. The forcing intensity is tuned by changing the amplitude of the excitation. The deformation of the plate is measured using a high speed Fourier transform profilometry technique [7,20] providing movies of the deformation over about  $1 \text{ m}^2$  (i.e., half the total surface of the plate) that are resolved both in time and space. The recording frame rate is varied between 5000 and 10 000 frames/s depending on the forcing intensity.

*Numerical simulation.*—The Föppl-von Kármán equations (1) are simulated with forcing, and dissipation by a pseudospectral algorithm with a second-order Runge-Kutta scheme and antialiasing [14] similar to that used in Ref. [4]. Resolutions are up to  $768^2$  grid points to ensure a full development of the wave spectrum. Physical parameters are chosen to be comparable to those of the experiment. The simulated plate is  $2 \times 2 \text{ m}^2$  in physical units. Forcing is chosen to mimic the experimental one: the linear modes around  $k = 5\pi$  are forced resonantly at their linear frequency (close to 30 Hz as in the experiment). Linear dissipation is implemented in two ways: first, a Lorentz dissipation (the dissipation time scale is decaying as a Lorentzian with the wave number  $k$ ) as measured in the experiment [9]. Such numerical simulations with realistic parameters have been shown to reproduce the observations for weakly nonlinear waves [14]. Another dissipation (called transparent dissipation in the following) is implemented: dissipation is acting only at the highest wave numbers of the simulation ( $k > 200\pi$ ). This enforces a constant flux of energy in the inertial (transparent) range between the forcing at  $k \approx 5\pi$  and the dissipation at  $k > 200\pi$  consistent with the framework of the WTT.

*Analysis of Fourier spectra.*—Figure 1 shows the power spectra of the deformation of the steel plate for several forcing intensities for the experiment, numerical simulations with realistic dissipation and with transparent dissipation. All cases show the emergence of a new regime with a steeper spectrum at low wave number. The simulation shows a behavior very close to the experiment and is similar to the numerical results of Ref. [15]. The experimental study confirms that the effect is present in real plates and is not an artifact of the Föppl-von Kármán equation driven out of their domain of validity. The simulation with transparent dissipation is in agreement with the theoretical prediction at low forcing intensity and shows the same departure at low wave number and strong forcing. Thus, the observed change in spectrum is not due to a peculiar dissipation of real plates.

*Description of the new regime.*—Figure 2 shows snapshots of the deformation of the simulated plate in the case

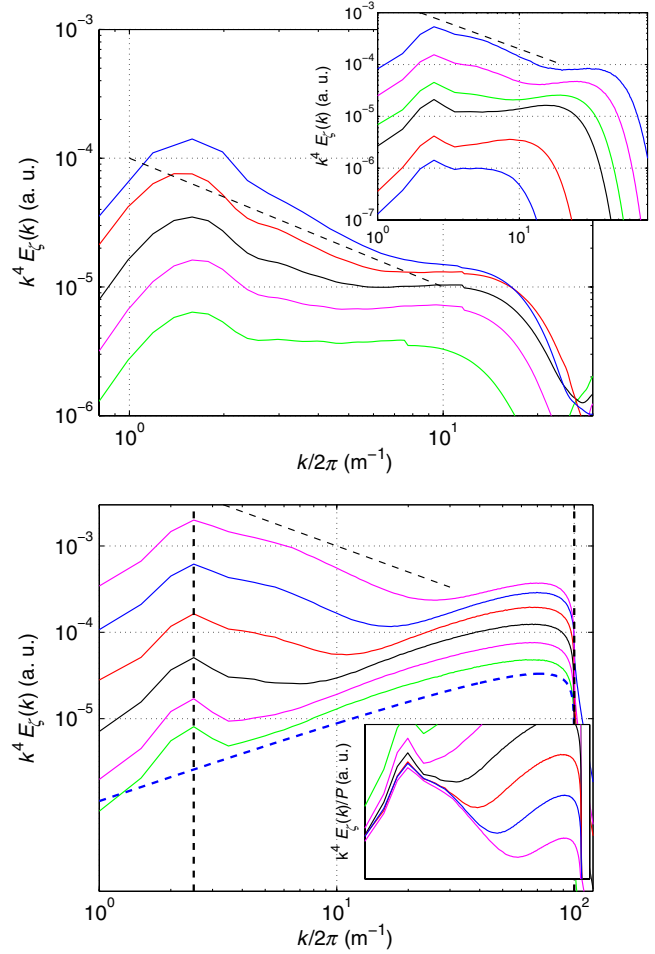


FIG. 1 (color online). Spectra of the plate deformation (multiplied by  $k^4$ ). Forcing intensity is increasing from the bottom curve to the top curve. Top figure: experiment (forcing magnitude in arb. units: 0.5, 0.75, 1, 1.25, 1.5 from bottom to top). Inset: numerics with Lorentz dissipation mimicking the experimental dissipation (the forcing magnitude is increasing by a factor of 2 between each curve from bottom to top). The dashed line is a  $1/k$  decay. Bottom figure: numerical simulations with transparent dissipation. The left vertical line marks the forcing wave number, and the right vertical line shows the lower wave number of the dissipation range. The lower dashed line stands for the theoretical prediction for weakly nonlinear wave turbulence [4]. The forcing magnitude is increasing by a factor of 2 between each curve from bottom to top. Inset: spectrum rescaled by  $P$ .

of transparent dissipation for the lowest and the strongest forcing intensities. The magnitude of the deformation is over one order of magnitude larger at the strongest forcing. The shape of the plate is very different in the two situations: at small forcing, where the KZ spectrum is observed, the deformation looks like a rock surface and it appears extremely rough. On the other hand, at strong forcing, it resembles rather crumpled paper [21] and seems smoother at first glance (note, however, the different vertical range between the two plots). The large scale deformation is made of folds with sharp crests that form ridges

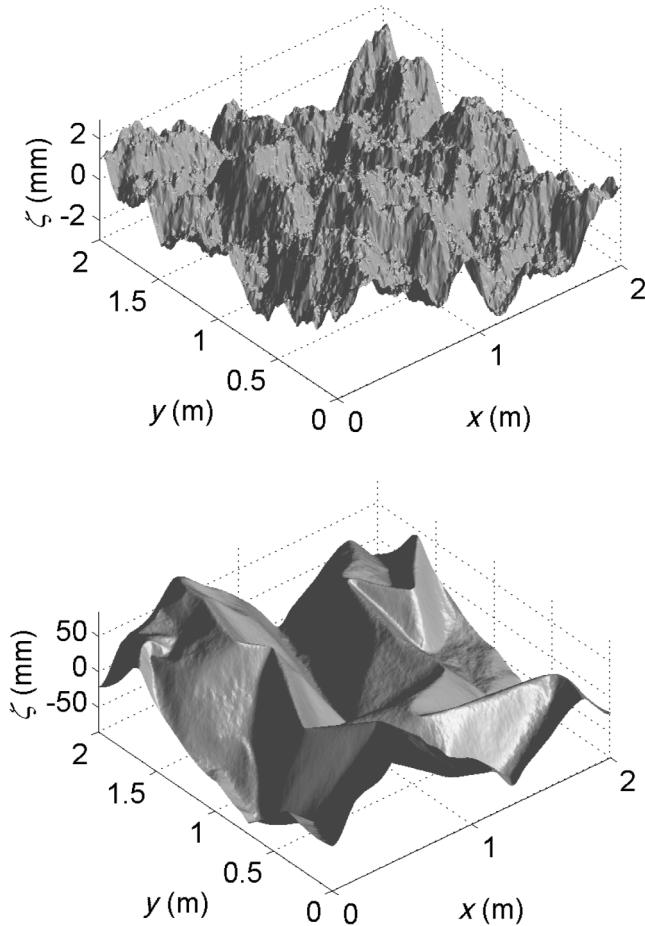


FIG. 2. Snapshots of the deformation for numerical simulations with transparent dissipation. Top: smallest forcing amplitude. Bottom: largest forcing amplitude.

connecting developable cones (*D* cones) [22] responsible for the fast decay of the spectrum at small  $k$ . *D* cones and ridges are singular structures that concentrate the stress resulting from the deformation of the plate. The difference between the two snapshots reveals a transition from a diffuse stress to a concentrated stress [21] in a dynamical regime. Indeed the folds are actually dynamical structures that form, move for a while, and then disappear: we refer to this new regime of vibration as dynamical crumpling by analogy with the static crumpling of an elastic sheet. The ridges and *D* cones are regularized at small scales by the nonlinearity of the von Kármán equations [23]. In fact, as can be seen from the spectra in Fig. 1, the small scale deformations are still following the KZ solution so that one can consider that small scale turbulent wave fluctuations still exist on top of the large scale folds.

A more detailed observation of the deformation shows that on a single fold, the slopes are almost constant. This feature is also characteristic of static crumpling [21]. This observation is supported by the pictures of the magnitude of the gradient displayed in Fig. 3 at the weakest and strongest forcing. At weak forcing, the picture of the

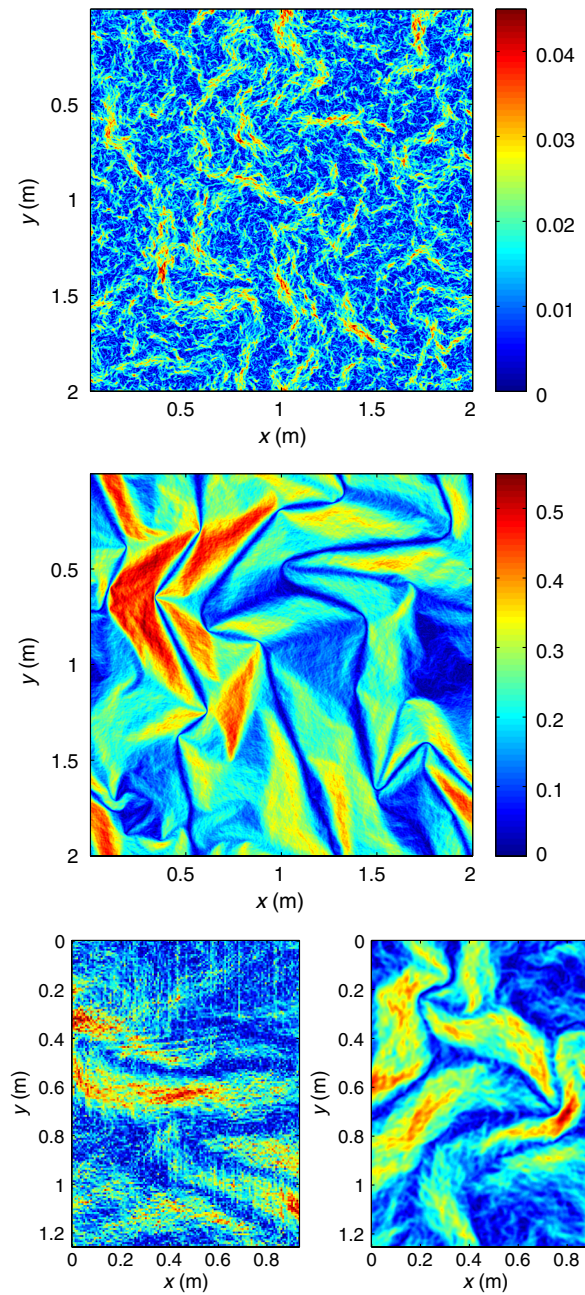


FIG. 3 (color online). Magnitude of the gradient of the deformation. Numerical simulations with transparent dissipation: Top: smallest forcing amplitude. Center: largest forcing amplitude. Bottom: comparison of the experiment at strongest forcing (left) and numerical simulation with Lorentz dissipation (right). The simulation picture has been truncated to the size of the experimental picture.

gradient shows a small scale filamentary structure. At strong forcing, the gradient follows a very different spatial repartition: the largest values of the gradients are structured in stripes separated by very narrow “valleys” of zero gradient corresponding to the ridges. The comparison between the experiment and the numerical simulations

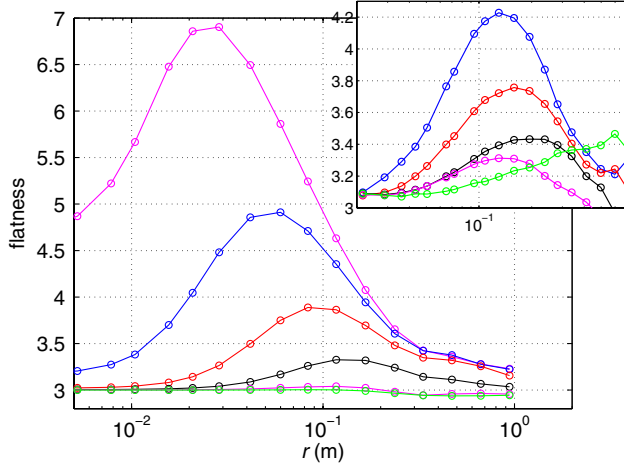


FIG. 4 (color online). Flatness of gradient increments [Eq. (5)]. Main figure: numerics with transparent dissipation. Inset: experiment. The forcing magnitude increases from bottom to top.

with the empirical Lorentz dissipation at strong forcing shows that similar features are observed for real plates.

*Analysis of spatial increments of the gradient.*—A way to quantify the previous observations is to study the evolution of spatial increments of the spatial derivatives of the deformation

$$\delta g_x(r) = \frac{\partial \zeta}{\partial x}(\mathbf{R} + r\hat{\mathbf{x}}) - \frac{\partial \zeta}{\partial x}(\mathbf{R}), \quad (4)$$

where  $\hat{\mathbf{x}}$  is the unit vector along the  $x$  direction and  $\mathbf{R}$  a position in the  $xy$  plane. We expect the probability distribution of such increments to change significantly between the weak forcing regime and the strong one reflecting the emergence of intermittency. The flatness of the increments

$$F(r) = \langle \delta g_x(r)^4 \rangle / \langle \delta g_x(r)^2 \rangle^2 \quad (5)$$

provides an indicator of the departure from a Gaussian statistics (for which the flatness is equal to 3). Figure 4 shows the evolution of the flatness as a function of the forcing intensity for the experiment and for the numerics with the transparent dissipation case (here the average is over  $\mathbf{R}$  and time). At weak forcing, the flatness is close to 3 reflecting Gaussian statistics at all scales. Thus, no intermittency is observed in this regime; the statistics are the same at all scales. At strong forcing, the flatness is close to 3 both at the small and large scales, but at intermediate scales of the order of 10 cm the flatness takes values significantly larger than 3 (over 4 in the experiment and over 7 in the numerics). The statistics are thus changing with scale reflecting the presence of intermittency. The length scale associated to the maximum flatness corresponds roughly to the width of the large gradient stripes observed in Fig. 3 (the forcing wavelength is about 40 cm). By contrast, the flatness of the deformation or velocity

increments (not shown) is almost unchanged when the forcing is increased and remains close to 3.

*Discussion.*—We have identified that the new dynamical regime is made of moving ridges delimited by  $D$  cones. It enters into the spectrum at small wave numbers (starting from the forcing scale) and invades more and more scales as the amplitude of the forcing increases. A surface dominated by ridges only would develop an elevation spectrum  $E_\zeta(k) \propto 1/k^4$  [4,24], i.e., slightly different from the KZ spectrum (3) but not as steep as our observations. Modeling the cone by the simple deformation relation  $\zeta = rf(\theta)$  (singular at  $r = 0$ ) yields the following contribution to the deformation spectrum [4]  $E_\zeta(k) \propto 1/k^5$ , in good agreement with the observed behavior at large scales as displayed in Fig. 1 where the slope  $1/k$  is indicated for large forcing amplitudes. The regularization of the singularity gives a correction to this scaling at short scales, which is eventually not relevant in the observation since the spectrum is then dominated by the usual wave turbulence contribution. The observed intermittency is clearly related with the existence of these structures.

We would like to argue here that the emergence of this new dynamical regime is related to the breakdown of wave turbulence. A key ingredient in the WTT is that the nonlinearities remain “weak” at each scale or equivalently that the nonlinear time scale is much larger than the linear one. Since the magnitude of the wave amplitude evolves with the scale within the cascade, the ratio between these two time scales usually varies between the forcing and the dissipative scales. Then, if the inertial range is wide enough the nonlinearity becomes significantly strong and intermittency develops either at the largest or smallest scales [16,17]. This regime of strong turbulence due to the breakdown of weak turbulence leads to different dynamical properties for which a general theory is still missing. Comparing the linear time ( $\tau_L$  due to the wave oscillation) to the nonlinear time ( $\tau_{NL}$  due to the nonlinear interactions between the waves) at each scale for the KZ spectrum yields, following [4,17] (up to the logarithmic correction terms)

$$\frac{\tau_L}{\tau_{NL}} \sim \frac{P^{2/3}}{k^4}. \quad (6)$$

The wave number scaling of this ratio shows that the wave turbulence hypothesis of time separation between the fast wave oscillation and asymptotic nonlinear contribution fails at large scales and for high forcing amplitudes. Here the singularities dominate the spectrum at low wave numbers consistently with the above argument. At higher wave numbers, the scale separation  $\tau_{NL} \gg \tau_L$  is still satisfied so that weak turbulence can proceed. The spectrum of the new regime is scaling as  $P/k^5$ , as seen in Fig. 1 (bottom), suggesting that the number of singularities increases also linearly with  $P$  [24].

Finally, it can be noted that experiments on water surface waves (gravity-capillary waves) in which singularities are indeed observed [25] also show a spectrum that scales linearly with  $P$  in place of the Kolmogorov-Zakharov scaling [26,27] ( $P^{1/3}$  for gravity,  $P^{1/2}$  for capillary). It may be due to the fact that the observed regime of water waves is dominated by singularities, consistent with the observation that the scaling in wave number is not the one predicted by WTT for water waves.

This research was supported by the ANR Grant No. TURBULON 12-BS04-0005.

---

\*nicolas.mordant@ujf-grenoble.fr

- [1] V. E. Zakharov, V. S. Lvov, and G. Falkovich, *Kolmogorov Spectra of Turbulence* (Springer, Berlin, 1992).
- [2] A. C. Newell and B. Rumpf, *Annu. Rev. Fluid Mech.* **43**, 59 (2011).
- [3] S. Nazarenko, *Wave Turbulence* (Springer, Berlin, 2011).
- [4] G. Düring, C. Josserand, and S. Rica, *Phys. Rev. Lett.* **97**, 025503 (2006).
- [5] A. Boudaoud, O. Cadot, B. Odille, and C. Touzé, *Phys. Rev. Lett.* **100**, 234504 (2008).
- [6] N. Mordant, *Phys. Rev. Lett.* **100**, 234505 (2008).
- [7] P. Cobelli, P. Petitjeans, A. Maurel, V. Pagneux, and N. Mordant, *Phys. Rev. Lett.* **103**, 204301 (2009).
- [8] N. Mordant, *Eur. Phys. J. B* **76**, 537 (2010).
- [9] B. Miquel and N. Mordant, *Phys. Rev. Lett.* **107**, 034501 (2011).
- [10] B. Miquel and N. Mordant, *Phys. Rev. E* **84**, 066607 (2011).
- [11] L. Landau and E. Lifshitz, *Theory of Elasticity* (Pergamon, New York, 1959).
- [12] M. Amabili, *Nonlinear Vibrations and Stability of Shells and Plates* (Cambridge University Press, Cambridge, England, 2008).
- [13] T. Humbert, O. Cadot, G. Düring, C. Josserand, S. Rica, and C. Touzé, *Europhys. Lett.* **102**, 30002 (2013).
- [14] B. Miquel and N. Mordant (to be published).
- [15] N. Yokoyama and M. Takaoka, *Phys. Rev. Lett.* **110**, 105501 (2013).
- [16] A. Newell and V. Zakharov, *Phys. Lett. A* **372**, 4230 (2008).
- [17] A. C. Newell, S. Nazarenko, and L. Biven, *Physica (Amsterdam)* **152–153D**, 520 (2001).
- [18] G. Düring, A. Picozzi, and S. Rica, *Physica (Amsterdam)* **238D**, 1524 (2009).
- [19] P. Cobelli, A. Przadka, P. Petitjeans, G. Lagubeau, V. Pagneux, and A. Maurel, *Phys. Rev. Lett.* **107**, 214503 (2011).
- [20] P. J. Cobelli, A. Maurel, V. Pagneux, and P. Petitjeans, *Exp. Fluids* **46**, 1037 (2009).
- [21] T. Witten, *Rev. Mod. Phys.* **79**, 643 (2007).
- [22] E. Cerda and L. Mahadevan, *Proc. R. Soc. A* **461**, 671 (2005).
- [23] M. Ben Amar and Y. Pomeau, *Proc. R. Soc. A* **453**, 729 (1997).
- [24] E. Kuznetsov, *JETP Lett.* **80**, 83 (2004).
- [25] E. Herbert, N. Mordant, and E. Falcon, *Phys. Rev. Lett.* **105**, 144502 (2010).
- [26] E. Falcon, C. Laroche, and S. Fauve, *Phys. Rev. Lett.* **98**, 094503 (2007).
- [27] M. Berhanu and E. Falcon, *Phys. Rev. E* **87**, 033003 (2013).